

# A Self-Consistent Numerical Magnetohydrodynamic (MHD) Model of Helmet Streamer and Flux-Rope Interactions: Initiation and Propagation of Coronal Mass Ejections (CMEs)

S. T. Wu and W. P. Guo

Center for Space Plasma and Aeronomic Research and  
Department of Mechanical and Aerospace Engineering  
The University of Alabama in Huntsville  
Huntsville, Alabama

We present results for an investigation of the interaction of a helmet streamer arcade and a helical flux-rope emerging from the sub-photosphere. These results are obtained by using a three-dimensional axisymmetric, time-dependent ideal magnetohydrodynamic (MHD) model. Because of the physical nature of the flux-rope, we investigate two types of flux-rope; (1) high density flux-rope (i.e. flux-rope without cavity, Wu *et al.*, 1996), and (2) low density flux rope (i.e. flux rope with cavity, Guo and Wu 1996). When the streamer is disrupted by the flux-rope, it will evolve into a configuration resembling the typical observed loop-like Coronal Mass Ejection (CMEs) for both cases. The streamer-flux rope system with cavity is easier to be disrupted and the propagation speed of the CME is faster than the streamer-flux rope system without cavity. Our results demonstrate that magnetic buoyancy force plays an important role in disrupting the streamer.

## 1. INTRODUCTION

Coronal Mass Ejections (CMEs) were first observed by the OSO-7 white light coronagraph in the 1960's. Space and ground-based observations established CMEs as an important component of solar coronal and interplanetary physics. This fascinating feature has the speed range of less than  $100 \text{ km s}^{-1}$  to more than  $1,000 \text{ km s}^{-1}$ , and up to  $10^{16} \text{ g}$  of coronal plasma with accompanying magnetic field being ejected away from the sun. They are believed to be the cause of interplanetary shocks and geomagnetic storms [Kahler, 1992; Gosling, *et al.* 1991]. A number of studies [Kahler, 1987; Hundhausen, 1993; Dryer, 1994] give some insight, till now, the physical mechanism which causes the CME initiation and propagation is still to be understood.

In the late 70's and early 80's, theoretical efforts to study the dynamics of CMEs were treated as an initial boundary value problem in the context of magnetohydrodynamics (MHD) simulations [Nakagawa *et al.*, 1978; 1981; Steinolfson *et al.*, 1978; Wu *et al.*, 1978, 1982;]. Their work in this period focused on the dynamical response of the corona to the thermal pulse introduced at the coronal base. Their initial states were static coronae with open or closed potential magnetic fields. The thermal pulse added to this idealized

background state was believed to be released by magnetic-to-thermal energy conversion during a flare. Dryer *et al.*, [1979] made a comparison directly with a particular CME event using Skylab-observed flare parameters as input. This approach was questioned by Sime *et al.*, [1984] because of the lack of several of important observed characteristics that were seen in four Skylab CMEs.

Observations during the mid-80's found that CMEs appear to leave the solar surface earlier than the onset of associated flares [Harrison, 1986], and CMEs seemed to be more closely associated with erupting prominences than with flares [Kahler *et al.*, 1989]. Recently, it is widely held that it is the destabilization of large-scale coronal magnetic fields that initiate CMEs [Hundhausen, 1993].

The evolutionary progress for the modeling of CMEs has been made which can be summarized as follows: the "first-generation" modeling work, [Wu, *et al.* 1978; 1982; Steinolfson, *et al.*, 1978, Nakagawa, *et al.*, 1978, 1981] the initial coronae were usually assumed to be static corona with potential or force-free fields. Observations found that many CMEs originate from disruption of large-scale quasi-static structures in the coronal helmet-streamers [Illing and Hundhausen, 1986]. Hence, in the "second-generation" modeling work, coronal helmet streamers were, and are presently, considered to be suitable as an initial state to study CME initiation. Steinolfson, Suess and Wu [1982] first constructed a self-consistent numerical helmet streamer solution including the solar wind using a relaxation method. The importance of the initial corona in CME simulations was pointed out by Steinolfson and Hundhausen [1988]. They constructed three initial coronal models and showed that only the heated helmet streamer can reproduce the major observed characteristics of loop-like CMEs. However, they still used a thermal driver as in the "first generation" studies. Using a magnetic driver, Guo *et al.*, [1991] also reproduced the major observed characteristics of loop-like CMEs in an ordinary helmet streamer. Recently, Wang *et al.*, have shown again that the pre-event model atmosphere plays a key role in the simulation of CMEs.

An additional solar driver mechanism was also recognized because of the fact that photospheric shear can store magnetic free energy in coronal magnetic fields. Accordingly, Wu *et al.*, [1983] performed the first numerical 2D MHD simulation of coronal response due to photospheric line-tied footpoint motion. More numerical works [e.g. Mikic' *et al.*, 1988; Biskamp and Welter, 1989] demonstrated that shearing may cause the coronal magnetic field to erupt.

Wu *et al.*, [1991] demonstrated a scenario of arch-filament eruption due to photospheric shearing which may lead to the initiation of CMEs. In a more recent

simulation, Linker and Mikic [1995] studied the dynamics of a helmet streamer when photospheric shearing is imposed. They found that the streamer erupts when a critical shear is exceeded. However, it takes an unrealistically-long time for the shear to exceed the critical value. Thus, two important points emerged during this "second generation" of numerical studies: (1) an appropriate steady-state helmet streamer had to be constructed; and (2) a variety of solar "drivers" demonstrated potential mechanisms for causal CME generation.

A fundamental theoretical issue of the energy source of CMEs has been discussed in the recent work of Aly [1984, 1991], Sturrock [1991], Low [1994] and Low and Hundhausen [1995]. Aly [1984, 1991] and Sturrock [1991] showed that if a force-free magnetic field is anchored to the surface of the sun, it cannot have an energy in excess of that in the corresponding fully open configuration. Low [1994] and Low and Hundhausen [1995] proposed that magnetic energy in the form of detached magnetic fields with cross-field currents may be the source of the total mass ejection energy. When we look at some observations, there are clear indications that helmet streamers may contain detached magnetic structures in their closed region.

Recently, we have extended our two-dimensional MHD planar model [Wu, Guo and Wang, 1995] to investigate the dynamical evolution of a coronal streamer containing a detached magnetic structure (bubble) in its closed field region to a three-dimensional axisymmetric geometry [Wu, Guo and Dryer, 1996] which enables us to study the dynamical response of a helmet streamer to the emergence of a helical magnetic flux-rope as proposed by Low [1994]. In this study, we shall use this model to investigate the dynamical interactions for a helmet streamer and a flux-rope with different properties. The models for the streamer and flux-rope system will be described in section 2. Numerical results are given in Section 3. Finally the concluding remarks will be included in Section 4.

## 2. MODELS FOR THE STREAMER AND FLUX-ROPE SYSTEM

According to observations, the helmet streamer reflects a global scale coronal magnetic field topology which consists of three parts; the high density dome, the low-density cavity and prominence within the cavity. Low [1994] suggested that this global scale coronal magnetic field topology could be represented by a two-flux magnetic system; (1) the cavity contains a detached magnetic flux-rope running above polarity inversion line anchored at two ends in the photosphere, and (2) the streamer arcade in the other direction linking bipolar regions as shown in Figure 1. Low and Hundhausen

[1995] have constructed an analytical solution without solar wind emphasized on the magnetic topology of quiescent prominences.

Recently, Guo and Wu [1996] have constructed a numerical MHD solution to represent the present scenario which is a quasi-static helmet streamer containing a flux rope with cavity (i.e. low density flux rope) in its closed field region. This solution is obtained based on our previous solution of streamer-high density flux rope as described by Wu et al. [1996]. Since the methods to construct these solutions are elsewhere [Wu et al., 1996; Guo and Wu, 1996], we only describe the physical models for these two cases in the following:

### *2.1 Streamer-Flux Rope System Without Cavity*

This case is a helmet streamer containing a high density flux-rope in its closed field region. Observationally, it will show that there is a bright core in the streamer. Figure 2 shows the numerical solution for (a) magnetic field lines and velocity vectors, and (b) polarization brightness which is obtained by the equation for the Thompson scattering of photospheric light using computed coronal density from the model output. This numerical solution is obtained by solving a set of standard ideal magnetohydrodynamic equations in the three-dimensional axisymmetric geometry using the relaxation method [Steinolfson, et al., 1982, Wu, et al., 1995, 1996]. The physical parameters at the solar surface are  $n_0 = 3.2 \times 10^8 \text{ cm}^{-3}$ ,  $T_0 = 1.8 \times 10^6 \text{ K}$ ,  $B_0 = 2.0 \text{ G}$ . The center of the flux rope has  $B_\phi = 0.67 \text{ Gs}$ ,  $\beta = 1.9$ .

### *2.2 Streamer-Flux Rope System With Cavity*

This is the case for low density rope which is obtained by simultaneously decreasing density and increasing the strength of the azimuthal component of the magnetic field ( $B_\phi$ ) of the quasi-static solution of the streamer-flux rope without cavity. The final solution is a quasi-static helmet streamer containing a flux rope with cavity. The physical parameters at the solar surface are the same as given in section 2.1, but the flux rope is different. At the center of the flux rope,  $B_\phi = 0.97$  and  $\beta = 0.12$ . The magnetic field lines, velocity vectors, and polarization brightness for this case are shown in Figure 3. By comparing Figures 2 and 3, we immediately recognize that the core of the high density flux-rope is much brighter in contrast to the low density flux-rope which shows void regions at the core of the streamer. It also shows that the plasma beta ( $\beta$ ) is much smaller for the low density flux-rope in comparison to the high density flux-rope.

## 3. NUMERICAL RESULTS

In order to understand the dynamical interactions of streamers and these two types of flux rope systems, we

have performed self-consistent numerical MHD computations using three-dimensional axisymmetric ideal MHD equations [Wu et al. 1996] with those cases mentioned in the previous section as the initial state. To initiate the evolutionary computation we increase the strength of the azimuthal component of the magnetic field  $B_\phi$  of the flux rope as such:

$$B_\phi^{n+1} = B_\phi^n \left( 1 + \delta \left( 1 - \frac{r^*}{0.85r_f} \right) \right), \dots \quad (1)$$

where  $r_f$  is the radius of the flux-rope,  $\delta$  is the arbitrary constant related to the magnitude of the increasing field strength,  $r^*$  is the distance between the center of the flux rope and the point where the strength of the  $B_\phi$  is raised with  $r^* < 0.85 r_f$  for this study, finally, the superscript “n” indicates the time step. Once the flux rope starts to move upward, we stop increasing  $B_\phi$  and let  $B_\phi$  be determined by the MHD equations. Then, we watch the evolution, the results for these two cases are summarized in the following.

For the purpose of making direct comparison of these two cases, we have set up the magnetic energy contents in each of these two types of streamer-flux rope systems for two different values of the prescribed  $B_\phi$ . To implement this situation, we simply give two different values of  $\delta$  in Eq. (1). For illustration of this process and understanding of the physical consequences, we have tailored our choice of “ $\delta$ ” into two categories: (1) fast propagation and (2) slow propagation events. It was determined that when  $\delta = 0.0045$ , it lead to a fast propagation event and the slow event corresponding  $\delta = 0.0015$  which is one third of the values of the fast propagation event. Figure 4 shows the position of the flux-rope center versus time for these two values of  $\delta$  and two types of streamer-flux rope systems. The magnetic energy referred to the magnetic energy of the corresponding potential field for these two values of  $\delta$  and two types of streamer-flux rope system is shown in Figure 5. For  $\delta = 0.0045$ , we increase  $B_\phi$  by 2 hours for the streamer-flux rope with cavity and 3.1 hours for the streamer-flux rope without cavity. This made the magnetic energy for the two cases almost the same, as shown in Figure 5a. For  $\delta = 0.0015$ , the corresponding times are 4 hours and 8 hours. The magnetic energy for these two cases are shown in Figure 5b. By examining these results, we made the following observations:

(1) the streamer-flux rope system with cavity responds to the emerging flux perturbation much faster than the streamer-flux rope system without cavity as shown in Figure 5. Figure 4 also shows that the propagation speed for the streamer-flux rope system

with cavity is higher than the structure without cavity (i.e.  $232 \text{ km s}^{-1}$  versus  $155 \text{ km s}^{-1}$  for  $\delta = 0.0045$ ). This is understandable, because, the structure with cavity has less mass and stronger magnetic field in the system which triggers the magnetic buoyancy force into play as we can observe by comparison of Figures 6 and 7. As we have suggested [Wu, Guo and Wang, 1995] that the streamer-bubble system becoming non-equilibrium is due to the nonlinear interactions of the Lorentz, pressure, and gravitational forces. In the present streamer-flux rope system with cavity, it shows that the mass is less and the field is stronger. These factors will cause activation of the magnetic buoyancy force and less gravitation pull down which enables the streamer-flux rope system with cavity to easily become non-equilibrium.

(2) By observing the results shown in Figure 4 and 5, the effects on the streamer-flux rope system with and without cavity due to the strength of emerging flux are clearly demonstrated. That is, the streamer structure with cavity are much more fundamental to the occurrence of coronal mass ejections (Figure 6) as suggested by Low [1994]. It is worth noting, that, the CME is propagating in front of the flux rope, the speed is much faster than the speed measured at the center of the flux rope because there is local expansion of flux rope (Figure 7) due to the buoyant force. In the present calculation, we show that CME loop front speed is  $\sim 305 \text{ km/s}$  and  $\sim 280 \text{ km/s}$ , respectively for the case with and without cavity of the fast event and  $\sim 250 \text{ km/s}$  and  $\sim 210 \text{ km/s}$  for the case with and without cavity of a slow event.

It is understood that if the simulated models are meaningful, they must exhibit simulated features which resemble observed characteristics. In order to examine the present models on this issue, we have constructed the polarization brightness for these two types of streamer-flux rope systems for  $\delta = 0.0045$  as shown in Figure 6. We note that the observed loop-like CMEs [Burkepile and St. Cyr, 1993] are simulated by the model of streamer-flux rope with cavity (Figure 6a). In the case of the streamer-flux rope system without cavity (Figure 6b), although the frontal loop is similar to observation, the inner part is a little different. Because this is a high density flux rope, the trailing edge of the flux-rope shows much brighter features than the loop-like CME itself. The void region shown in the core of the high density flux-rope is because of the increasing of  $B_{\phi}$  as we have prescribed.

For completeness, the evolution of the magnetic field topology and velocity vector for the streamer-flux rope system with and without cavity for the fast event ( $\delta = 0.0045$ ) are shown in Figures 7 and 8, respectively. By looking at magnetic field topology, the buoyancy

effects are clearly shown in the case of streamer-flux rope system with cavity.

#### 4. CONCLUDING REMARKS

In this study we have employed two models [Wu et al, 1996; Guo and Wu, 1996] to investigate the dynamical interactions of streamers and two types of flux ropes. On the basis of this simulation study, we may conclude:

1. The numerical results of the streamer-flux rope with cavity model has reproduced most of the three parts of the global coronal streamer feature as suggested theoretically by Low [1994].

2. The helmet streamer-flux rope system has more magnetic energy than the conventional streamer without flux rope. Because of its high magnetic energy content, the streamer-flux rope system is easily disrupted by disturbances, like what we used in this paper.

3. With the same magnetic energy contents, the model of streamer-flux rope system with cavity responds faster in comparison with the model without cavity. It is also shown that the propagation speed is higher with cavity than without cavity which demonstrates that magnetic buoyancy force played an important role in disrupting the streamer. For both cases, the erupted streamer-flux rope system reproduced the major observed characteristics of looplike CMEs.

4. This study shows that the fast event will produce magnetohydrodynamic shocks. We have not performed a detailed analysis for the physics of shock in the present study, but with a quick look at Figure 7, it clearly indicates that MHD fast shocks at the leading edge of the event and MHD slow shocks at the trailing edge of the event could be observed.

In summary, these two models are capable to perform quantitative analyses of the complex CME event and to predict the north-south change of  $B_z$ -component of interplanetary magnetic field (IMF) relative to CME events.

*Acknowledgments.* The work performed by STW and WPG is supported by NASA Grant NAG8W-4665 and NRL through USRA N00014-C-95-2058.

#### REFERENCES

- Aly, J. J., Some properties of force-free magnetic fields in infinite regions of space, *Astrophys. J.*, 283, 349, 1984.
- Aly, J. J., How much energy can be stored in a three-dimensional force-free magnetic field?, *Astrophys. J.*, 374, L61, 1991.
- Biskamp, D. and H. Wilter, Magnetic Arcade Evolution and Instability, *Solar Phys.*, 120, 49, 1989.
- Burkepile, J. T. and D. C., St. Cyr, A revised and expanded catalogue of mass ejections observed by the solar

- maximum mission coronagraph, NCAR/TN-369\_STR, 1993.
- Dryer, M., S. T. Wu, R. S. Steinolfson and R. M. Wilson, Magnetohydrodynamic models of coronal transients in the meridional plane. II. Simulation of the coronal transient of 1973 August 21, 227, 1059, 1979.
- Dryer, M., Interplanetary studies: Propagation of disturbances between the sun and the magnetosphere, *Space Sci. Rev.*, 67, 363, 1994.
- Gosling, J. T., D. J. McComas, J. L. Philips, and S. J. Borne, Geomagnetic activity associated with earth passage of interplanetary shock disturbances and coronal mass ejections, *J. Geophys. Res.*, 96, 7831, 1991.
- Guo, W. P., J. F. Wang, B. X. Liang and S. T. Wu, A numerical simulation of magnetically driven coronal mass ejections, in Z. Svestka, B. V. Jackson, and M. E. Machado (Eds.) "Eruptive Solar Flares", IAU Colloquium 133, 381, 1991.
- Guo, W. P. and S. T. Wu, A magnetohydrodynamic description of coronal helmet streamers containing cavity, *Astrophys. J.* (to be submitted).
- Harrison, R. A., Solar Coronal Mass Ejections and Flares, *Astron. Astrophys.*, 162, 283, 1986.
- Hundhausen, A. J., Sizes and locations of coronal mass ejections: SMM Observations from 1980 and 1984 - 1989, *J. Geophys. Res.*, 98, 13177, 1993.
- Illing, R. M. E. and A. J. Hundhausen, Disruption of coronal streamer by an eruptive prominence and coronal mass ejection, *J. Geophys. Res.*, 91, 10951, 1986.
- Kahler, S. W., Solar Mass Ejections, *Rev. Geophys.*, 25, 63, 1987.
- Kahler, S. W., N. R. Sheeley, Jr. and M. Liggett, Coronal mass ejections and associated X-ray flare durations, *Astrophys. J.*, 344, 1026, 1989.
- Kahler, S. W., Solar flares and coronal mass ejections, *Annu. Rev. Astron. Astrophys.*, 30, 113, 1992.
- Linker, J. A., and Z. Mikic', Disruption of a helmet streamer by photospheric shear, *Astrophys. J.*, 438, L45, 1995.
- Low, B. C., Magnetohydrodynamic processes in the solar corona: flares, coronal mass ejections, and magnetic helicity, *Phys. Plasmas*, 1, 1684, 1994.
- Low, B. C., and J. R. Hundhausen, magnetostatic structures of the solar corona. II. The magnetic topology of quiescent prominences, *Astrophys. J.*, 443, 818, 1995.
- Mikic', Z., D. C. Barnes, and D. D. Schnack, Dynamic evolution of a solar coronal magnetic field arcade, *Astrophys. J.*, 328, 830, 1988.
- Nakagawa, Y., S. T. Wu, and S. M. Han, Magnetohydrodynamics of atmospheric transients. I. Basic results of two-dimensional plane analyses, *Astrophys. J.*, 219, 314, 1978.
- Nakagawa, Y., S. T. Wu, and S. M. Han, Magnetohydrodynamics of atmospheric transients. III. Basic results of two-dimensional plane analyses, *Astrophys. J.*, 244, 331, 1981.
- Sime, D. G., R. M. MacQueen, and A. J. Hundhausen, Density disruption in looplike coronal transients: a comparison of observations and theoretical model, *J. Geophys. Res.*, 89, 2113, 1984.
- Steinolfson, R. S., S. T. Wu, M. Dryer, and E. Tandberg-Hanssen, Magnetohydrodynamic models of coronal

- transients in the meridional plane. I. The effect of the magnetic field, *Astrophys. J.*, 225, 259, 1978.
- Steinolfson, R. S., S. T. Suess, and S. T. Suess, The steady global corona. *Astrophys. J.*, 255, 730, 1982.
- Steinolfson, R. S., A. J. Hundhausen, *J. Geophys. Res.*, density and white light brightness in looplike coronal mass ejections: temporal evolution, 93, 14269, 1988.
- Sturrock, P. A., Maximum energy of semi-infinite magnetic field configurations, *Astrophys. J.*, 380, 655, 1991.
- Wang, A. H., S. T. Wu, and G. Poletto, Numerical modeling of coronal mass ejections based on various pre-event model atmosphere, *Solar Phys.*, 161, 365, 1995.
- Wu, S. T., M. Dryer, Y. Nakagawa and S. M. Han, Magnetohydrodynamics of atmospheric transients. II. two-dimensional numerical results for a model solar corona, *Astrophys. J.*, 219, 324, 1978.
- Wu, S. T., Y. Nakagawa, S. M. Han, and M. Dryer, Magnetohydrodynamics of atmospheric transients. IV. nonplane two-dimensional analyses of energy conversion and magnetic field evolution, *Astrophys. J.*, 262, 369, 1982.
- Wu, S. T., Y. Q. Hu, Y. Nakagawa, and E. Tandberg-Hanssen, induced mass and wave motions in the lower solar atmosphere. I. Effects of shear motion on flux tubes, *Astrophys. J.*, 266, 866, 1983.
- Wu, S. T., M. T. Song, P. C. H. Martens, and M. Dryer, Shear induced instability and arch filament eruption: A magnetohydrodynamic (MHD) numerical simulation, *Solar Phys.*, 134, 353, 1991.
- Wu, S. T., W. P. Guo and J. F. Wang, Dynamical evolution of a coronal streamer-bubble system, I. A self-consistent, planar magnetohydrodynamic simulation, *Solar Phys.*, 157, 325, 1995.
- Wu, S. T., W. P. Guo, and M. Dryer, Dynamical evolution of a coronal streamer-flux rope system. II. A self-consistent non-planar magnetohydrodynamic simulation, *Solar Phys.*, 1996 (in press).
- Wu, S. T. and W. P. Guo, Numerical MHD modeling of the solar driver for the destabilization of a coronal helmet streamer, *J. Adv. Space Res.*, 1997 (in press).

---

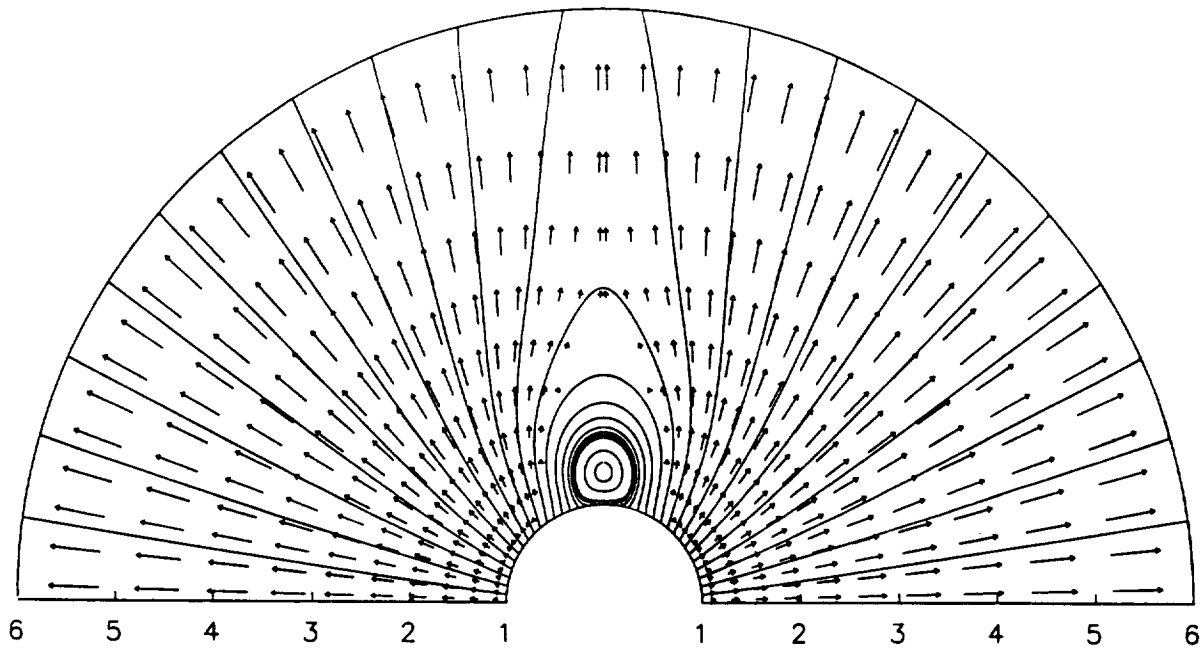
S. T. Wu and W. P. Guo, Center for Space Plasma and Aeronomic Research and Department of Mechanical and Aerospace Engineering, The University of Alabama in Huntsville, Huntsville, Alabama 35899 USA

**Figure 1.** Schematic representation of a streamer arcade and flux-rope system.

**Figure 2.** The computed (a) magnetic field lines and velocity vectors and (b) the corresponding polarization brightness for a streamer-flux rope system without cavity.

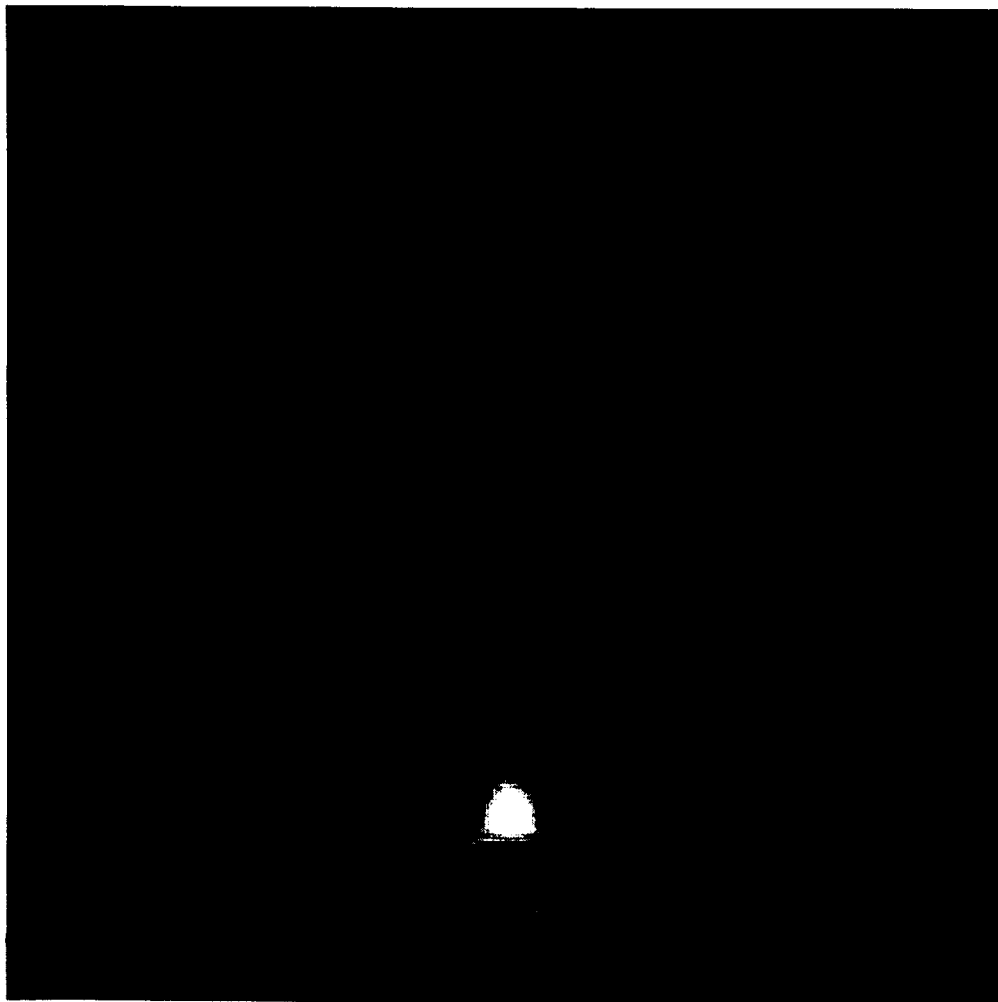
**Figure 3.** The computed (a) magnetic field lines and velocity vectors and (b) the corresponding polarization brightness for a streamer-flux rope system with cavity.



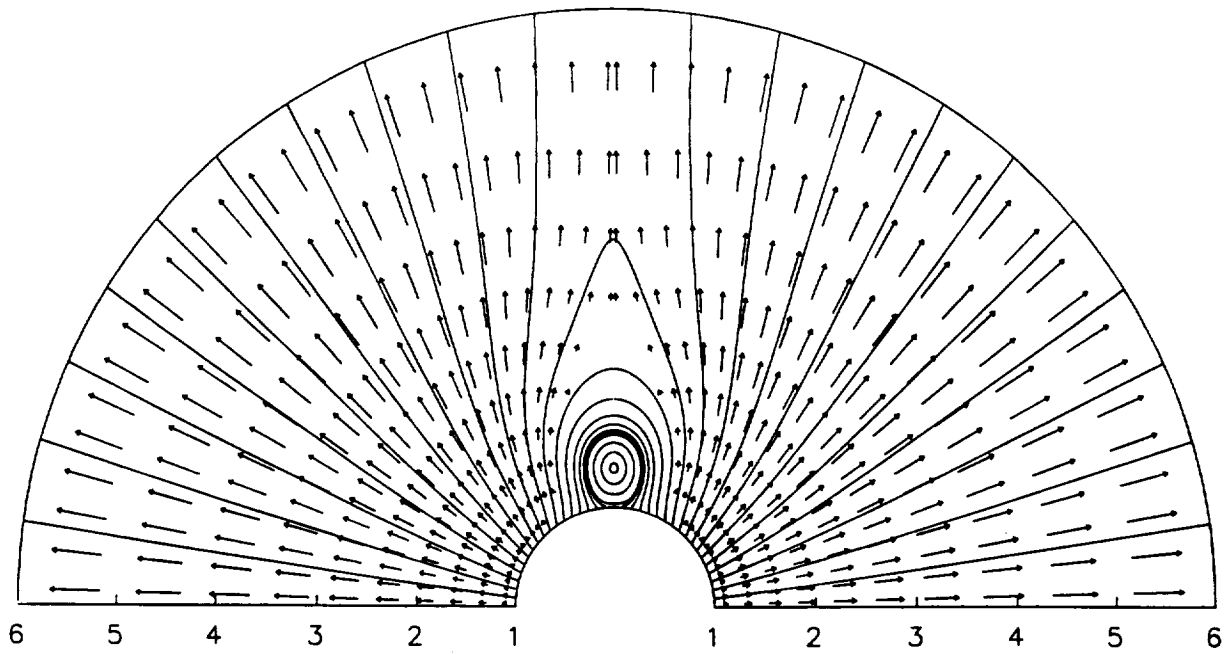


SOLAR RADII

(a)

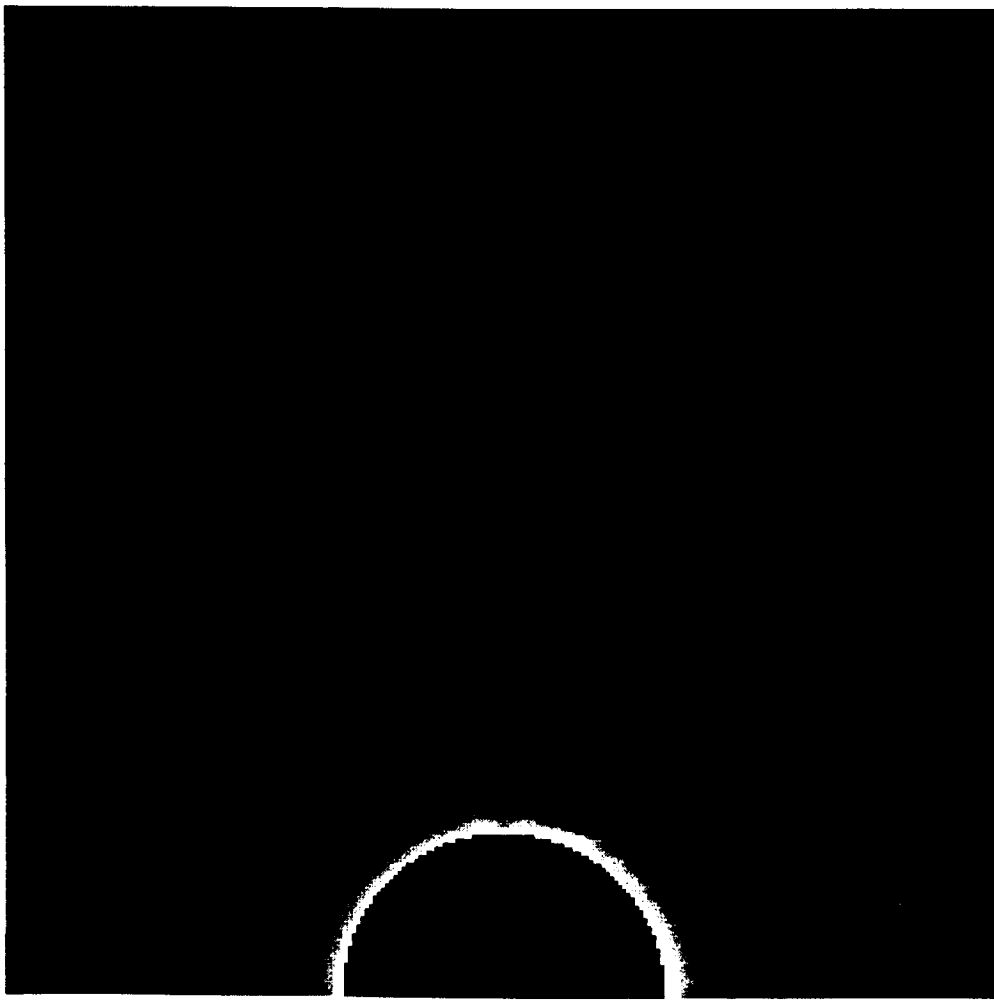


(b)



SOLAR RADII

(a)



(b)

Figure 4

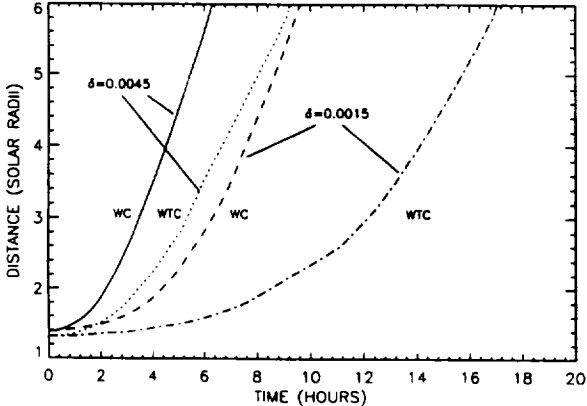
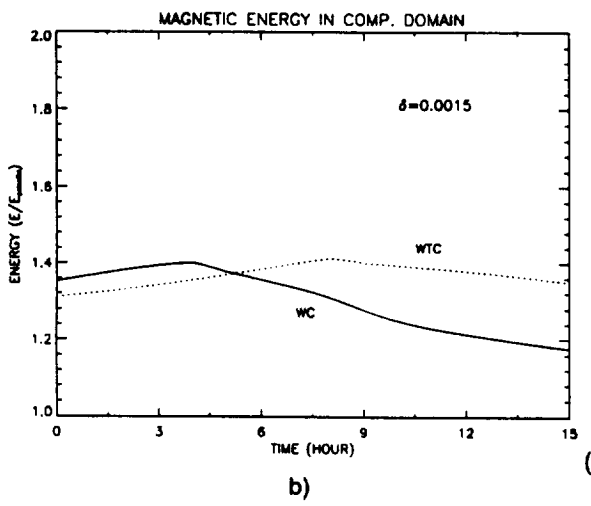
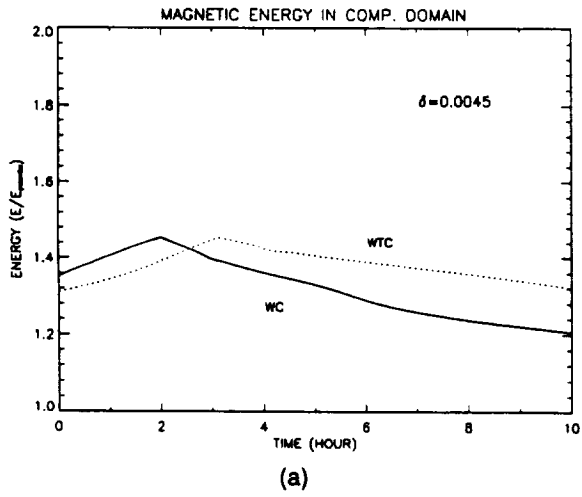
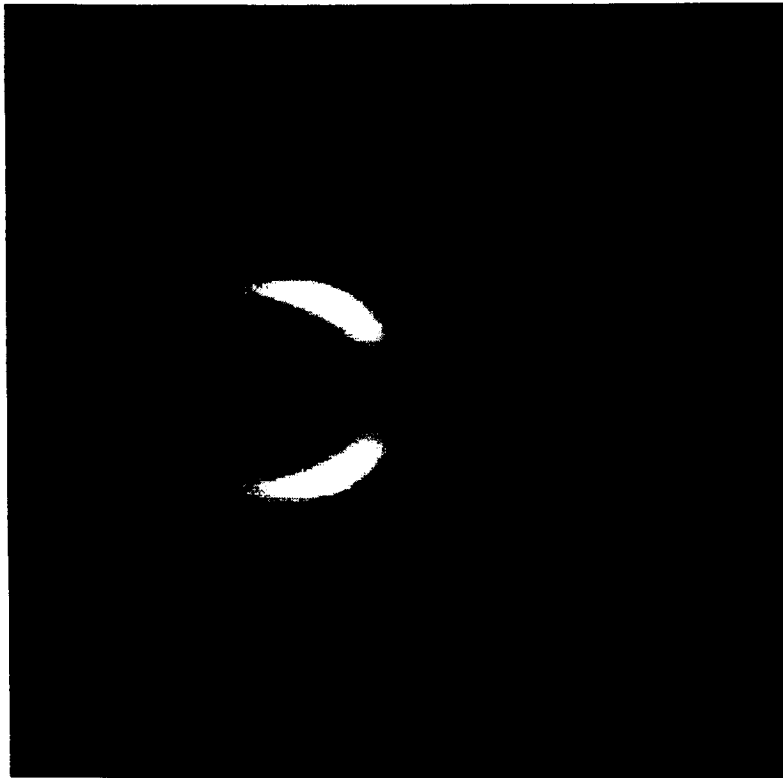
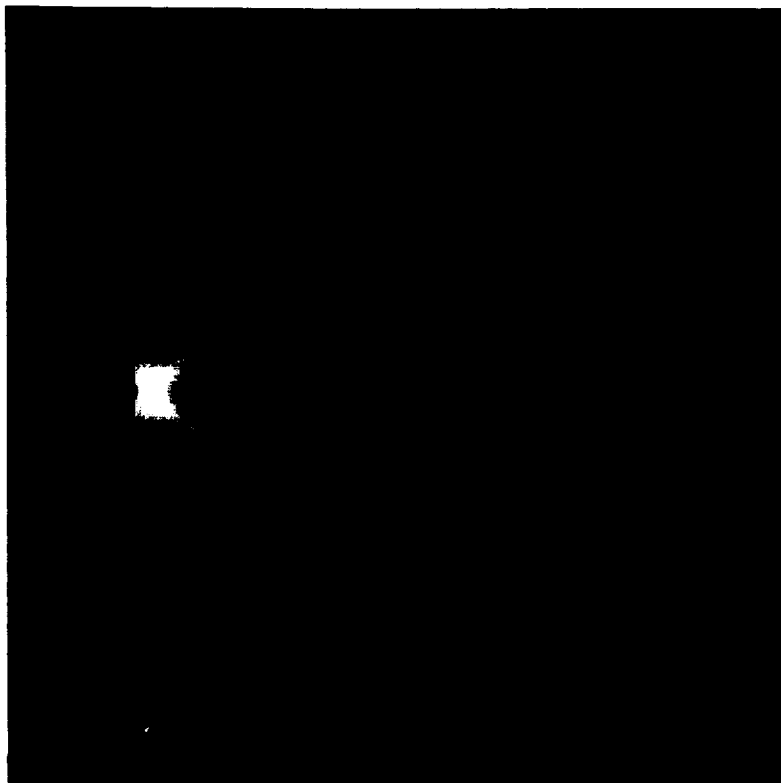


Figure 5





(a)



(b)

Figure 7

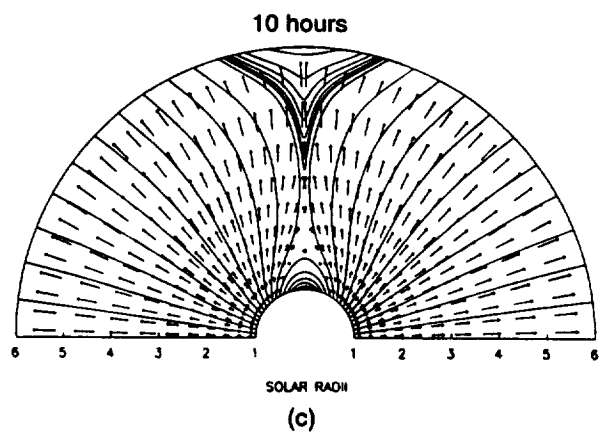
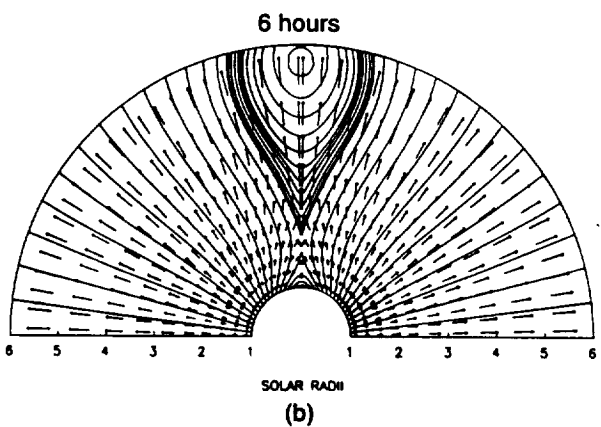
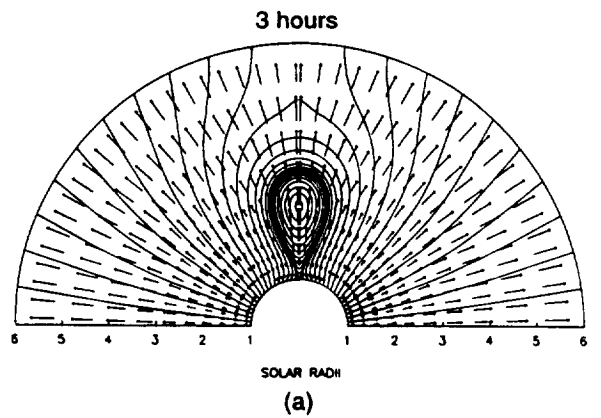
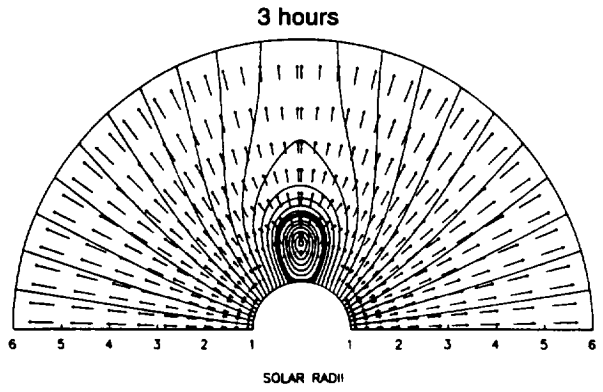
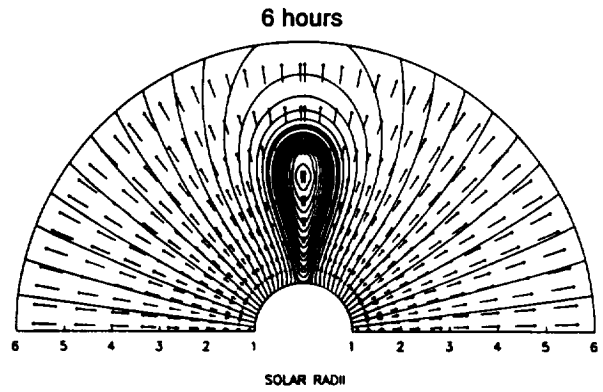


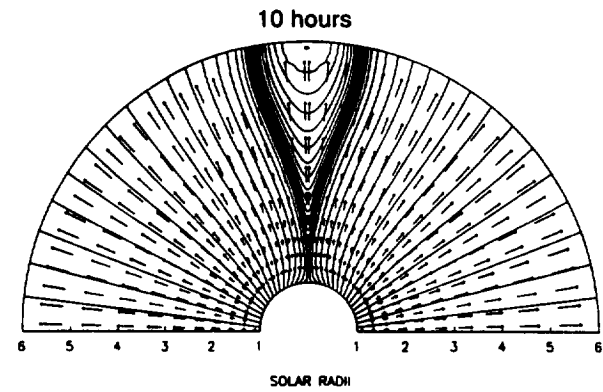
Figure 8



(a)



(b)



(c)

Figure 2

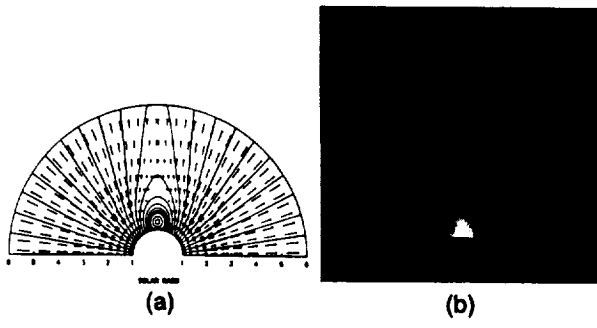


Figure 3

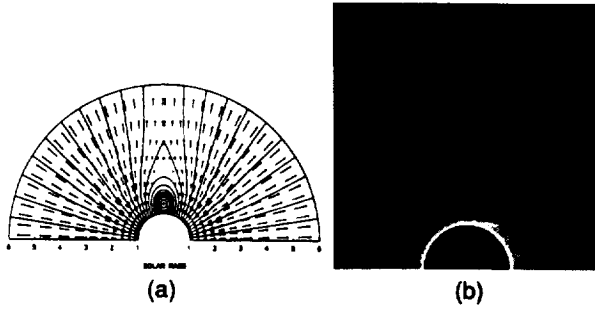


Figure 6

